Received: 4 December 2021 | Revised: 24 April 2022 | Accepted: 1 May 2022

DOI: 10.1002/qre.3128

RESEARCH ARTICLE

WILEY

An expanded case against synthetic-type control charts

Sven Knoth

Department of Mathematics and Statistics, Helmut Schmidt University, Hamburg, Germany

Correspondence
Sven Knoth, Department of Mathematics and Statistics, Helmut Schmidt University Hamburg, Holstenhofweg 85, 22043 Hamburg, Germany.
Email: knoth@hsu-hh.de

Abstract

During the last two decades, many new methods have appeared in statistical process monitoring with synthetic-type control charts being a prominent constituent. These charts became popular due to their simplicity and proclaimed excellent change point detection performance. Synthetic charts are nothing more than the application of well-known and long established runs rules. We show that better performance can be obtained by using exponentially weighted moving average (EWMA) charts. Expanding on some previous questioning articles, we critically reflect upon recently developed variants of synthetic-type charts in order to emphasize that there is no reason to apply this special class of control charts. This paper renews and extends criticism in order to respond to newly developed synthetic charts, called "revised" and "modified" by incorporation of further restrictions on the observations leading to an out-of-control signal. Furthermore, we demonstrate that "improved synthetic charts" (synthetic charts augmented with an outer Shewhart limit) perform weaker than EWMA–Shewhart chart combinations.

KEYWORDS

average run length, conditional expected delay, control chart, EWMA chart, statistical process monitoring, steady-state

1 | INTRODUCTION

The majority of the statistical tools we know as control charts were created in the 20th century. During the last years, however, numerous new concepts have been introduced. The synthetic chart, proposed by Wu and Spedding,[1,2] is an example. On the one hand, it provides a simple design and explicit solutions of the average run length (ARL) equation and related measures. The ARL is the expected number of samples or individual observations until the control chart declares that a change happened and lack of control was proclaimed.[3] The ARL comes in various types, where the most popular are the zero-state and steady-state ARL.[4] And on the other hand, in Wu and Spedding,[1] the synthetic chart was announced as superior in terms of the zero-state ARL, (unintentionally) concealing that it had an implicit head-start. So, Davis and Woodall[5] criticized this approach and suggested two key elements; enforce the steady-state ARL as performance measure, which captures potentially misleading side effects of head-starts and use the older runs rule, which differentiates between the change directions (called side-sensitive), as well with a head-start. This rather cautious critique did not block the

TABLE 1 Simplified version of Table 1 in Shongwe & Graham,[10] i. e. only 2-of-$H+1$ designs

#	Label	w/o head-start	w/ head-start
1	"True" synthetic	R_1 Derman and Ross[22a]	S_1 Wu and Spedding[1]
2	Side-sensitive	R_2 Klein[23]	S_2 Davis and Woodall[5]
3	Revised	R_3 Machado and Costa[24b]	S_3 Shongwe and Graham[10]
4	Modified	R_4 Antzoulakos and Rakitzis[25]	S_4 Shongwe and Graham[10]

[a]Derman and Ross[22]: "Probably the easiest way to construct a control chart that considers each subgroup average in relation to those around it is to define a chart that declares a process out of control if two successive averages differ from μ by more than $c\sigma$ for some value c."
[b]Machado and Costa[24]: "The transient states describe the position of the last L sample points; '1' means that the sample point fell below the LCL, '0' means that the sample point fell in the central region, and '1' means that the sample point fell above the UCL."

further development of synthetic charts. Instead, these charts have become popular. The more recent paper by Knoth[6] was much more explicit in its criticism. Nevertheless, synthetic charts remained highly attractive to researchers.

Rakitzis et al.[7] claimed that Knoth[6] considered only the original synthetic chart of Wu and Spedding.[1] This is partially correct, but the general message would be the same regardless, that is, synthetic charts and all their derivatives (published so far) are clearly dominated by older control charts. Here, we will utilize exponentially weighted moving average (EWMA) charts, which will be compared to all four types of synthetic-type charts. For the sake of a concise presentation, we touch only briefly on combinations of synthetic charts with Shewhart-type charts, which were called improved synthetic charts in Rakitzis et al.[7] Their "natural" counterpart is a Shewhart–EWMA combination.[8,9] We provide a thorough ARL (zero- and steady-state) analysis of eight (including charts without head-start like Shongwe and Graham[10]; in Knoth,[6] three synthetic-type charts were considered) different synthetic-type charts and the EWMA chart.

Before providing the outline of this contribution, we want to remind that applying runs rules started quite early. A rather incomplete list (all before 1960) is Shewhart,[11] Dudding and Jennett,[12] Wolfowitz,[13] Weiler,[14,15] Page,[16] WECO,[17] and Moore.[18] Most interestingly, already Page[16] provided an explicit result for the zero-state ARL of a primary synthetic chart without head-start combined with a Shewhart rule. His rule III is just what Rakitzis et al.[7] and other recent authors[7,19] called improved synthetic charts.

In Section 2, we describe all examined control charts in detail. Later, in Section 3, we elaborate upon the steady-state ARL concept, where some confusion has to be clarified. Our main results appear in Section 4, where we compare all the charts by considering the zero-state ARL, conditional expected delay (CED) and the steady-state ARL. Finally, we assemble our conclusions in Section 5.

2 | CLASSIFICATION SCHEME OF SYNTHETIC-TYPE CHARTS

As Rakitzis et al.[7] and others mentioned, the constitutive element of a synthetic chart is that two warnings or signals are needed to trigger the actual alarm. These two signals should not be too *"far away from each other."* Thus, synthetic charts are special runs (or scan) rules charts, because they could be expressed as 2-of-$H+1$ runs rules, with $H = 1, 2, ...$, cf. to Davis and Woodall[5] and Bersimis et al.[20] Differently from Rakitzis et al.,[7] we consider not only the head-start versions. Instead, following Shongwe and Graham[10,21] and Bersimis et al.,[20] we investigate common and head-start synthetic-type charts. In Table 1, we list the eight synthetic-type charts with their initial reference.

Besides Table 1, which is a simplified and reduced version of Table 1 in Shongwe and Graham,[10] we want to provide some more constructional details. For simplicity, we assume individual normally distributed observations with mean μ and standard deviation σ (more details in the next section). We set $H = 3$ as an example. Between two signals resulting from two observations beyond the limits, there must be at most two "unobtrusive" observations to trigger an alarm. For "true" synthetic charts (in the narrower sense), it is not important whether the two signals are raised on the same side of the chart, whereas the remaining three designs require signals on the same side.

In Figure 1, we plotted the center line at the in-control mean μ_0 and limits at $\mu_0 \pm k\sigma_0$. Here, σ_0 represents the in-control standard deviation, which is assumed to be constant and known. The design parameter k controls the detection behavior and is typically chosen to achieve a predefined in-control ARL. Pattern #1 in Figure 1 would trigger an alarm only for chart #1. The next pattern raises an alarm for the common 2-of-4 runs rule, where the lower signal has no impact on the final alarm. Chart #3 requires that the observations enclosed by the two upper signals reside between the limits. Later, we will see that there are only small performance differences between these latter two chart designs. The most restrictive design

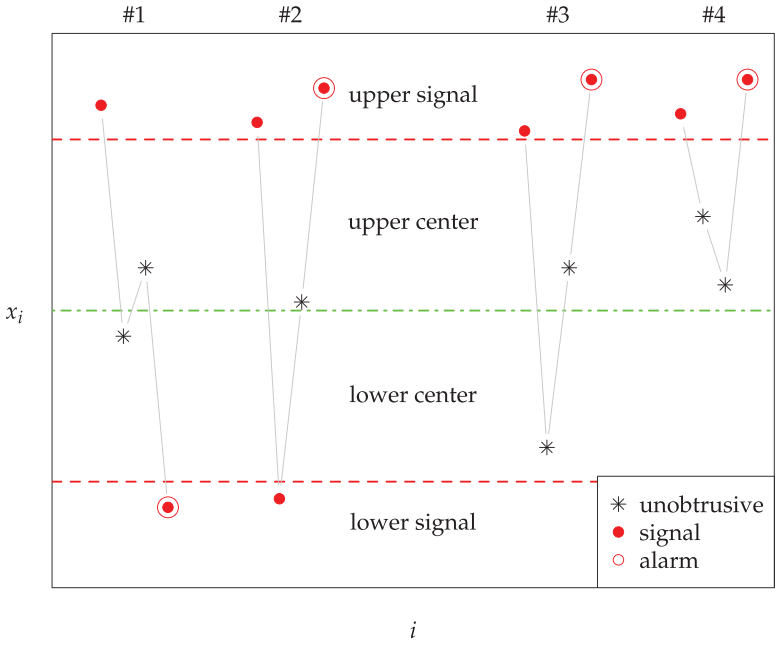

FIGURE 1 Four observations that form an alarm pattern for four different synthetic-type charts with $H = 3$

TABLE 2 Number of transient states, 2-of-$H + 1$ rules, see Table 1

#	w/o head-start	w/ head-start
1	DR: $H + 1$	WS: $H + 1$
2	KL: $H^2 + H + 1$	DW: $H^2 + 2H + 1$
3	MC1: $2H + 1$	MC2: $3H + 1$
4	AR: $2H + 1$	MSS: $4H$

is #4, where the in-between observations have to be on the same side as the signaling points. The patterns are chosen so that pattern #4 flags an alarm for all four charts, whereas pattern #3 signals only for chart #1, #2, #3, and so forth. Of course, these different patterns demand distinct values of k, namely $2.2087 > 2.0760 > 2.0723 > 1.9642$ for #1, …, #4, respectively, for $H = 3$ and in-control ARL 500. Note that the k values for charts with head-start would be slightly larger.

With a head-start one presumes that the data point just before monitoring was started would trigger a signal. Hence, we need only one further signal to raise an alarm. Except for #1, however, we have to know whether the signal was above the upper or below the lower limit. This problem is dealt with pragmatically, that is, given the first observed signal, one would assume that the hidden signal was on the same side, providing kind of a wildcard head-start[1]. There are some side effects to the Markov chain modeling, except for #1, of course. Specifically, we have to introduce further states of the chain that are related to this particular starting behavior. In Table 2, we indicate the resulting number of transient states we obtain for the underlying Markov chain model, cf. to Shongwe and Graham.[10] We added as well the chart labels used in Shongwe and Graham[10] and Bersimis et al.[20]

The smallest value, $H + 1$, is known from Davis and Woodall.[5] The latter reported as well the largest value in Table 2, observed for the DW chart, namely $(H + 1)^2$. From the latter size, one can straightforwardly derive the number for the general KL chart, that is, $H^2 + H + 1$ (Knoth[6] dealt with three synthetic-type charts: WS, KL, and DW). The dimension $2H + 1$ was given in Machado and Costa.[24] The remaining values are given in Shongwe and Graham.[10]

Before continuing with the competitor EWMA, we want to mention that the recent Chakraborti and Rakitzis[26] labeled the synthetic-type charts differently. Their S_1 and S_3 correspond to WS (our S_1) and DW (our S_2), respectively. The remaining two in Chakraborti and Rakitzis,[26] S_2 and S_4, are just the latter combined with a Shewhart alarm rule.

As already mentioned, we utilize the common EWMA[27] chart with varying limits as the main competitor to all the synthetic-type charts. Picking an appropriate value for the smoothing constant $0 < \lambda \leq 1$ (we favor here 0.25 and 0.1), we

[1] Davis and Woodall[5]: *"The initial state is 0±; that is, the most recent observation at the onset of monitoring is considered to be beyond control limits on both sides of the center line."*

have the following sequence of EWMA statistics[8,28] and signaling time:

$$Z_0 = \mu_0, \quad Z_i = (1-\lambda)Z_{i-1} + \lambda X_i, \quad i = 1, 2, \ldots, \tag{1}$$

$$L_E = \min\left\{ i \geq 1 : |Z_i - \mu_0| > c_E \sqrt{(1-(1-\lambda)^{2i})\frac{\lambda}{2-\lambda}}\sigma_0 \right\}. \tag{2}$$

Fortunately, there are numerical algorithms[29–31] for calculating all performance metrics we use (see next section). We apply the routines in the R package `spc`.[32]

3 | STEADY-STATE ARL AND OTHER MEASURES

As mentioned in the previous section, we consider an independent series $X_1, X_2, \ldots$ following a normal distribution with mean μ and standard deviation σ. To incorporate a potential change, we apply the change point (τ) model

$$\mu = \begin{cases} \mu_0 = 0, & t < \tau \\ \mu_1 = \delta, & t \geq \tau \end{cases} . \tag{3}$$

Regarding the standard deviation (variance) we make the common assumption that it is known, $\sigma = \sigma_0 = 1$ (otherwise normalize the X_t), and it remains constant.

We let L represent the run length (stopping time), which is the number of observed X_i values until an alarm is raised. The expected values of L for the two situations $\tau = 1$ and $\tau = \infty$ constitute the well-known zero-state ARL, cf. to Page[33] and Crosier.[4] The control charts are set up to yield a predefined in-control ARL, that is, $E_\infty(L) = A$ for some suitably large number A (here we set $A = 500$). For a given control chart design, it is a common task to determine out-of-control ARL values, $E_1(L)$, for specified values of δ. The resulting ARL profiles are typically used to judge the detection performance over a range of changes δ and to compare charts to each other.

Besides the simple case $\tau = 1$ in Equation (3), we determine the series of CEDs

$$D_\tau = E_\tau(L - \tau + 1 \mid L \geq \tau) \quad , \tau = 1, 2, \ldots$$

and its limit, the conditional steady-state ARL

$$\mathscr{D}_1 = \lim_{\tau\to\infty} D_\tau.$$

Both $\{D_\tau\}$ and $\mathscr{D}_1$ are functions of δ. For all charts considered here (EWMA and synthetic-type), the series $\{D_\tau\}$ converges quickly to $\mathscr{D}_1$. Besides $\mathscr{D}_1$, one can utilize the cyclical steady-state ARL $\mathscr{D}_2$, which incorporates restarts after getting a false alarm. See Taylor,[34] Crosier,[4] and the recent paper by Knoth[35] for more details. It is defined as follows:

$$\mathscr{D}_2 = \lim_{\tau\to\infty} E_\tau(L_\star - \tau + 1)$$

$$\text{with} \quad L_\star = L_1 + L_2 + \cdots + L_{I_\tau - 1} + L_{I_\tau} \quad \text{and} \quad I_\tau = \min\left\{ i \geq 1 : \sum_{j=1}^{i} L_j \geq \tau \right\}.$$

Thus, after some number of false alarms ($L_1, L_2, \ldots, L_{I_\tau - 1}$ as the observation counts to the next false alarm), the first true alarm appears at observation $L_\star \geq \tau$. The term $L_\star - \tau + 1$ denotes the resulting detection delay. Of course, the restarting pattern influences the actual value of $\mathscr{D}_2$.

Denoting by $\mathbb{Q}$ the transition matrix of transient states, $\mathbb{I}$ the identity matrix and $\mathbf{1}$ a vector of ones, we start with the classical ARL (vector $\boldsymbol{\ell}$) result of Brook and Evans[36]

$$\boldsymbol{\ell} = (\mathbb{I} - \mathbb{Q})^{-1}\mathbf{1},$$

and continue with some prerequisites for the steady-state vectors, cf. to Knoth.[35] In particular, we have

$$\varrho\boldsymbol{\psi}_1 = \mathbb{Q}'\boldsymbol{\psi}_1,$$
$$\boldsymbol{\psi}_2 = \left(\mathbb{I} - \mathbb{Q}'\right)^{-1}\boldsymbol{e}_1.$$

The first vector, $\boldsymbol{\psi}_1$, is just the left (positive) eigenvector corresponding to the dominant eigenvalue ϱ. The second one, $\boldsymbol{\psi}_2$, is the solution of a linear equation system with the unit vector $\boldsymbol{e}_1$ being its right-hand side, which consists of zeros except for the restart state, where a 1 is set. The equation for $\boldsymbol{\psi}_1$ was given in Brook and Evans,[36] whereas the $\boldsymbol{\psi}_2$ equation was included in Darroch and Seneta.[37] Both vectors will be normalized (i.e., $\mathbf{1}'\boldsymbol{\psi}_i = 1, i = 1, 2$). Then the two steady-state ARLs are calculated via $\mathscr{D}_i = \boldsymbol{\psi}_i'\boldsymbol{\ell}$, $i = 1, 2$ (exact for synthetic-type, approximation for EWMA). For chart S_1,[1] we have

$$p = p(k;\delta) = 1 - [\Phi(k-\delta) - \Phi(-k-\delta)] \quad , q = 1 - p \quad , r = p(1 - q^H), \tag{4}$$

with $\Phi()$ representing the cdf of the standard normal distribution. The following explicit solutions have been derived in Knoth.[6] Labeling the states of the underlying Markov chain with $0, 1, \ldots, H$, which count simply the number of unobtrusive observations after the last signal we obtain

$$\boldsymbol{\ell}' = \begin{array}{c} \begin{array}{ccccc} 0 & 1 & \ldots & H-1 & H \end{array} \\ \left(\begin{array}{ccccc} \frac{1}{r} & \frac{1+q^H(q^{-1}-1)}{r} & \ldots & \frac{1+q^H(q^{-(H-1)}-1)}{r} & \frac{1}{r}+\frac{1}{p} \end{array}\right), \end{array}$$

$$\boldsymbol{\psi}_1' = \begin{array}{c} \begin{array}{ccccc} 0 & 1 & \ldots & H-1 & H \end{array} \\ \left(\begin{array}{ccccc} s & \frac{q}{\varrho}s & \ldots & \left(\frac{q}{\varrho}\right)^{H-1}s & \frac{\varrho}{p}s \end{array}\right) \end{array} \quad , s = 1 - q/\varrho,$$

$$\boldsymbol{\psi}_2' = \begin{array}{c} \begin{array}{ccccc} 0 & 1 & \ldots & H-1 & H \end{array} \\ \left(\begin{array}{ccccc} p & pq & \ldots & pq^{H-1} & q^H \end{array}\right). \end{array}$$

Thereby, the eigenvalue ϱ is determined numerically, whereas the other parameters have been set in Equation (4). Recall that the restart for $\boldsymbol{\psi}_2$ is assumed to happen at state one, which refers to the head-start situation and results in $\boldsymbol{e}_1 = (1, 0, \ldots, 0)'$. Note that Wu et al.[38] utilized this restart state. However, Shongwe and Graham[21] considered $\boldsymbol{e}_1 = (0, \ldots, 0, 1)'$, which corresponds to the no head-start case. The resulting cyclical steady-state vector is

$$\boldsymbol{\psi}_3' = \frac{1}{2-q^H} \begin{array}{c} \begin{array}{ccccc} 0 & 1 & \ldots & H-1 & H \end{array} \\ \left(\begin{array}{ccccc} p & pq & \ldots & pq^{H-1} & 1 \end{array}\right). \end{array}$$

The vectors $\boldsymbol{\psi}_2$ and $\boldsymbol{\psi}_3$ differ in the entry for state H, namely q^H and 1, respectively, and in the normalizing constant, 1 and $1/(2-q^H)$, respectively. The impact to the resulting $\mathscr{D}_2$ value is not substantial. Shongwe and Graham[21] did not explain why they used a different head-start. Moreover, it remains as well unclear why they proposed two ways of calculating the cyclical steady-state vector. First, there are more than two approaches. Second, all these different procedures provide equal solutions (except for the scaling constant). For a detailed discussion refer to Knoth.[35] A more important problem, however, is the wrong result of both Shongwe and Graham,[21] and Machado and Costa,[24] for $\mathscr{D}_1$ (conditional), in particular for its steady-state vector ($\boldsymbol{\psi}_1$). By following the erroneous path in Crosier,[4] they obtained

$$\boldsymbol{\psi}_4' = \frac{1}{1+Hp} \begin{array}{c} \begin{array}{ccccc} 0 & 1 & \ldots & H-1 & H \end{array} \\ \left(\begin{array}{ccccc} p & p & \ldots & p & 1 \end{array}\right). \end{array}$$

First, note that Crosier[4] introduced the terms conditional and cyclical and he also provided Markov chain algorithms to calculate these steady-state ARLs. His procedure for the cyclical steady-state ARL is correct, although it is not the one indicated in Shongwe and Graham.[21] However, the approach to get the conditional steady-state ARL by following *"the matrix* $\mathbb{R}$ *… can be scaled up so that each row of the matrix sums to 1"* Crosier,[4] is wrong. For more details, we refer to Knoth.[35] The surprisingly simple $\boldsymbol{\psi}_4$ is the output of this wrong algorithm applied to the S_1 chart. We wonder why none

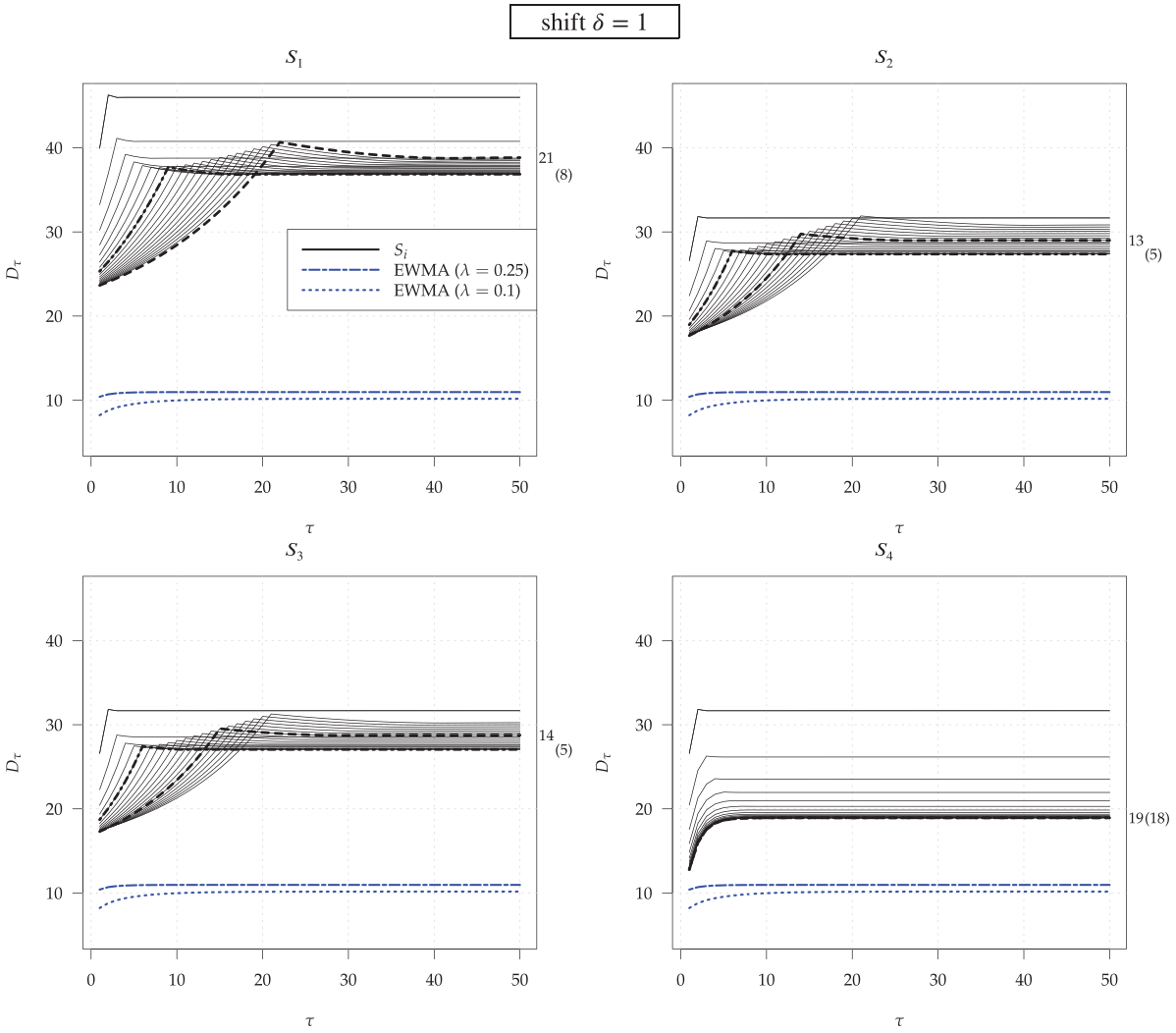

FIGURE 2 CED profiles D_τ for four synthetic-type charts with head-start, with $H = 1, 2, \ldots, 20$. The best scheme (zero-state and steady-state) is bolded (dashed and dash-dotted) lines. Two EWMA charts are included. All with in-control ARL 500

of the above authors questioned this nearly uniform distribution. The good news is that the numerical differences when using $\boldsymbol{\psi}_1, \ldots, \boldsymbol{\psi}_4$ are not large, see Appendix A. Therefore, it is not too restrictive to apply the conditional steady-state ARL $\mathscr{D}_1$ relying on $\boldsymbol{\psi}_1$ and the related CED D_τ for the rest of the paper. Note that neither Rakitzis et al.[7] nor Chakraborti and Rakitzis[26] touched on these subtle complications in their discussion of the steady-state ARL.

4 | COMPARISON STUDY

We start with a CED analysis of the four synthetic-type charts with a head-start. All considered control charts are designed to have an in-control ARL, $E_\infty(L)$, of 500. For the aforementioned charts, labeled as $S_1, \ldots, S_4$, we determined the CED D_τ for $\tau = 1, 2, \ldots, 50$. Moreover, we plot the CED profiles for $H = 1, 2, \ldots, 20$. We begin in Figure 2 with a shift of size $\delta = 1$. We display in addition to the 20 mentioned profiles two EWMA ($\lambda = 0.25$ and $= 0.1$) CED profiles.

First, we observe that the detection performance gets better as we progress from S_1 to S_4. Second, there is a pronounced difference between S_4 and the other synthetic-type charts. For the latter, there is a clearly identifiable CED maximum at $\tau = H + 1$. Later, we will learn about the root cause of this behavior (see Figure 7). The larger H, the sharper the increase is from $\tau = 1$ to $\tau = H + 1$. In case of S_4 for all $H = 1, \ldots, 20$, stability of the D_τ seems to be reached before $\tau = 10$. Looking at the actual numbers, we see the same $\tau = H + 1$ yielding the maximum. Nonetheless, the S_4 version could be sufficiently

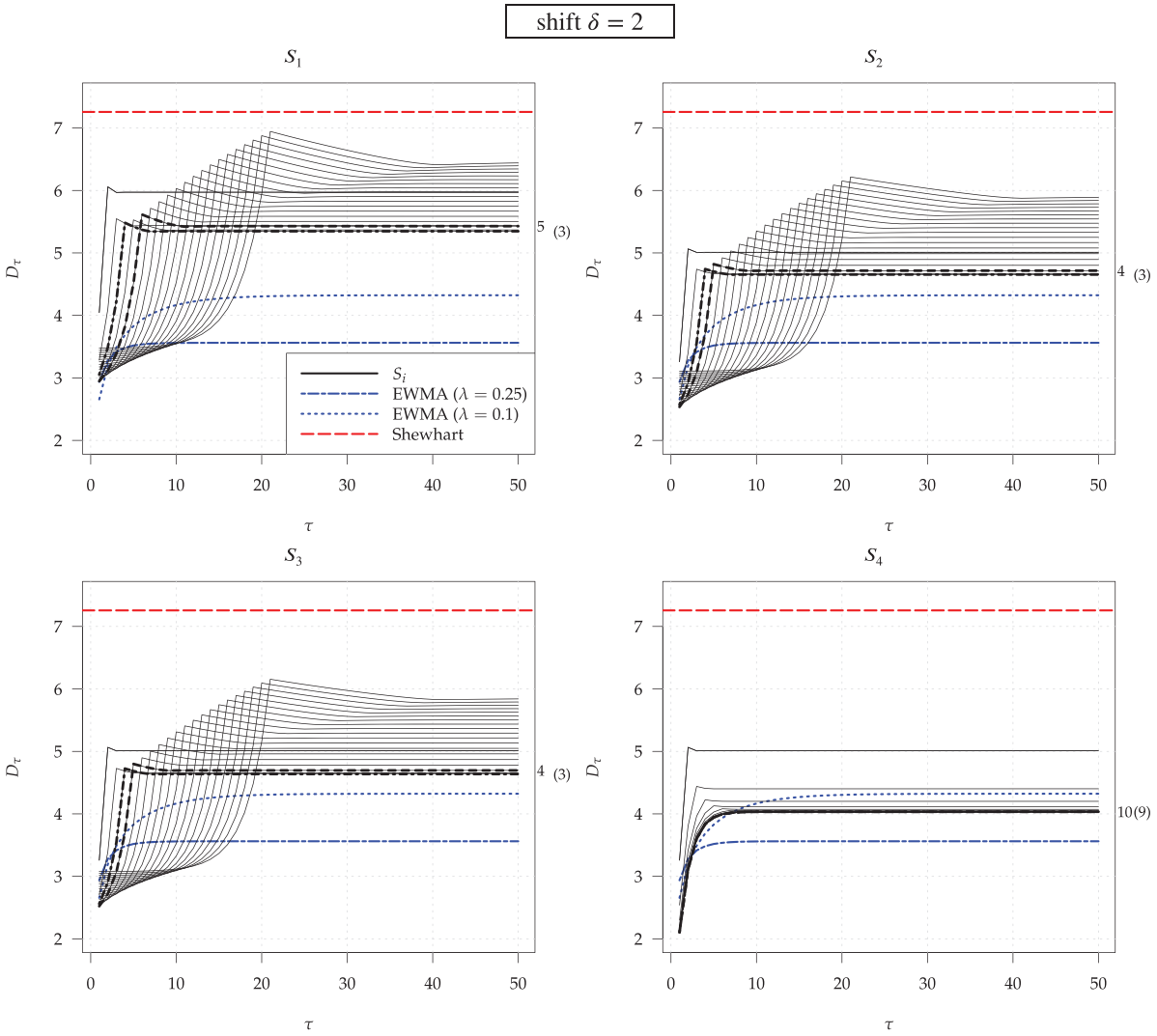

FIGURE 3 CED profiles D_τ for four synthetic-type charts with head-start, with $H = 1, 2, \ldots, 20$. The best scheme (zero-state and steady-state) is bolded (dashed and dash-dotted) lines. Two EWMA charts are included. All with in-control ARL 500

well characterized by the zero-state and the steady-state ARL, whereas for the others the inner maximum is important too, because it is considerably larger than the other two measures.

In Figure 2, we marked the profiles with the lowest zero-state and steady-state ARL (here we considered $H \leq 25$), by bold dashed and dash-dotted lines, respectively, and the related H value annotated on the right-hand margin. The H values for the minimum zero-state ARL ($H = 21, 13, 14$) are substantially larger than for the steady-state ones ($H = 8, 5, 5$), except for S_4 (values are quite similar: $H = 19$ and 18). For all synthetic charts with a head-start, the zero-state ARL is markedly smaller than the steady-state ARL. Therefore, judging these charts by only using the zero-state ARL values is misleading. From all synthetic profiles, we conclude that the steady-state ARL is a much more representative measure than the more common zero-state ARL, in particular for S_4. Turning to the established competitor, we consider the EWMA profiles (two-dash and dotted line for $\lambda = 0.25$ and $= 0.1$, respectively). These two profiles reside clearly below all synthetic-type chart counterparts. Thereby, the $\lambda = 0.1$ EWMA chart is slightly better than the $\lambda = 0.25$ one (will change for larger δ). The Shewhart chart ARL at $\delta = 1$ with a value of 54.58 is too large to be seen in Figure 2.

We conclude that for $\delta = 1$, the "old" EWMA control chart exhibits the best performance. Later, we will see that the version with $\lambda = 0.25$ does a good job for all considered shifts. For smaller shifts $\delta < 1$, the advantage of EWMA is even more pronounced, cf. to Appendix D Figure D.1. Before considering larger changes, we want to emphasize that S_2 and S_3 show nearly the same profiles, with a slight advantage for the latter.

For the larger change $\delta = 2$ (see Figure 3), there are some clear overlaps between the synthetic and EWMA profiles. However, for changes at $\tau > 15$ (note the in-control ARL is 500), the EWMA chart with $\lambda = 0.25$ is again the clear winner

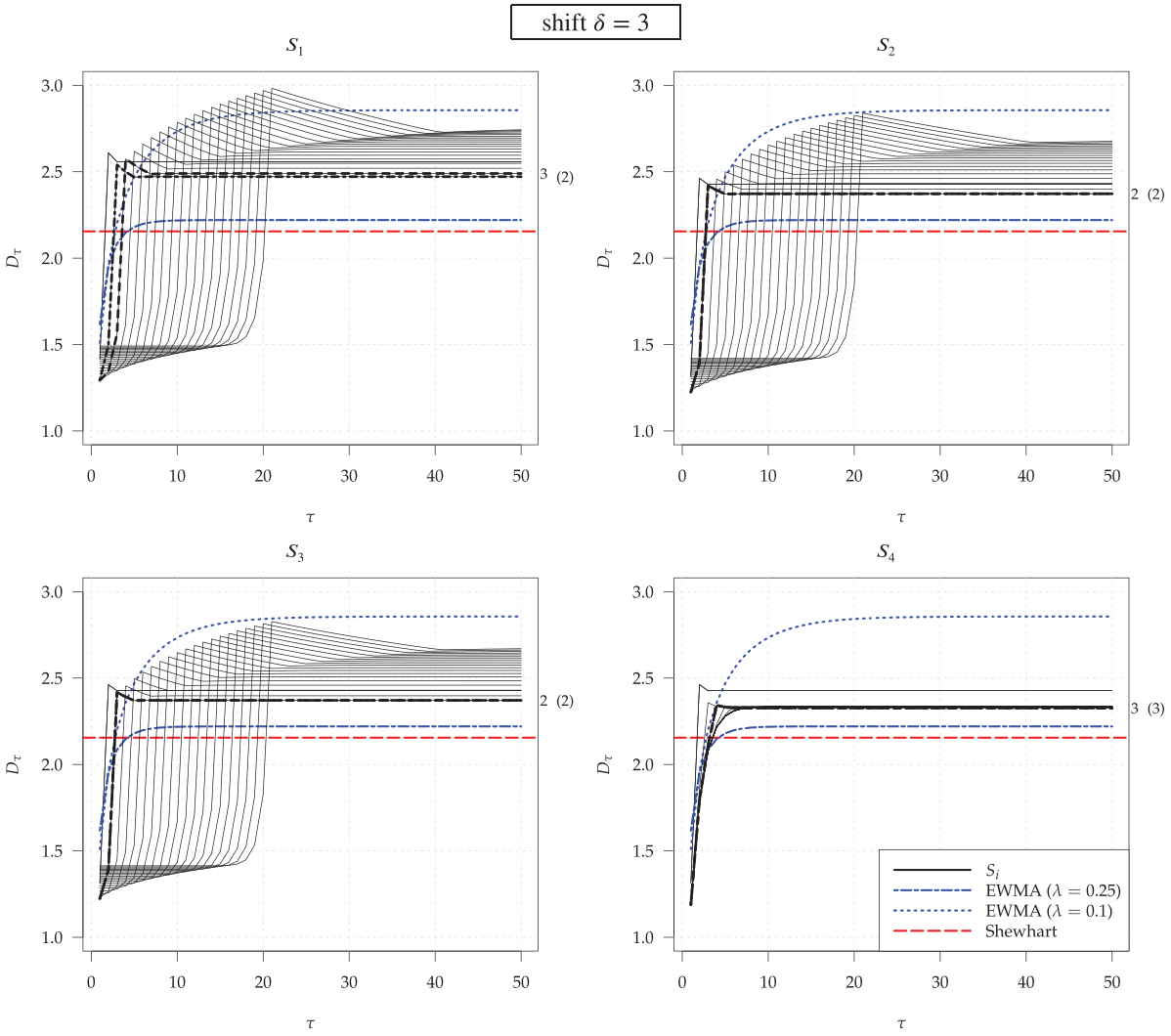

FIGURE 4 CED profiles D_τ for four synthetic-type charts with head-start, with $H = 1, 2, \ldots, 20$. The best scheme (zero-state and steady-state) is bolded (dashed and dash-dotted) lines. Two EWMA charts are included. All with in-control ARL 500

(for S_4, $\tau > 3$ suffices). Note that the synthetic-type chart (S_1, S_2, S_3) configurations, which perform better than EWMA for $5 \le \tau \le 15$, exhibit poor performance for later changes, $\tau \ge 20$, which removes them clearly from the competition. The EWMA chart with the smaller $\lambda = 0.1$ can compete with S_1, S_2, and S_3, but not with most of the S_4 designs. Thus, the actual competition is between the synthetic-type schemes and an EWMA chart with a mid-size λ. Before discussing the profiles of the former more in detail, we want to note that all charts behave better than the Shewhart chart (now its CED profile is visible). Except for S_4, the differences between the profiles and within them are much more pronounced than with $\delta = 1$. The optimal H values are now smaller than for $\delta = 1$, that is we obtain for the zero-state ARL $H = 5, 4, 4, 10$ and for the steady-state ARL $H = 3, 3, 3, 9$ for $S_1, \ldots, S_4$, respectively. It is interesting that nearly the same H value makes the considered ARL types minimal, per chart type. For all four synthetic-type charts, choosing $H \in \{4, 5, 6, 7\}$ seems to be a good choice. In summary, we conclude that for $\delta = 2$, EWMA ($\lambda = 0.25$) is the best performing chart with S_4 (and $H > 2$) in second place.

Next, we consider the change $\delta = 3$, where the Shewhart chart yields the smallest steady-state ARL. In Figure 4, we see similar patterns as before in Figure 3. Starting with S_1, S_2, and S_3, we observe the same (even much more) pronounced step shift of D_τ at $\tau = H + 1$. The best configuration, in terms of both ARL types, is either $H = 2$ or $= 3$. For these, the zero-state ARL (equal to D_1, of course) and the CED value D_2 are lower than for the EWMA ($\lambda = 0.25$) chart, whereas for $\tau > 2$, the latter chart exhibits the smallest D_τ values including its limit, the steady-state ARL. Thus, again the EWMA chart dominates these three synthetic-type charts. The same has to be said about S_4 and the EWMA ($\lambda = 0.25$) chart, except for D_3, where both feature similar values. For all four synthetic-type charts with head-start we encounter, in case of the optimal

TABLE 3 Optimal values of H for minimizing zero- and steady-state out-of-control ARL; in-control zero-state ARL is set to 500

δ	0.25	0.5	0.75	1	1.5	2	2.5	3	4	5
Zero-state										
R_4	12	15	17	17	14	8	4	3	2	2
S_4	12	15	18	19	15	10	6	3	2	2
Steady-state										
R_4	12	15	17	17	14	9	5	3	2	4
S_4	12	15	17	18	14	9	5	3	2	4

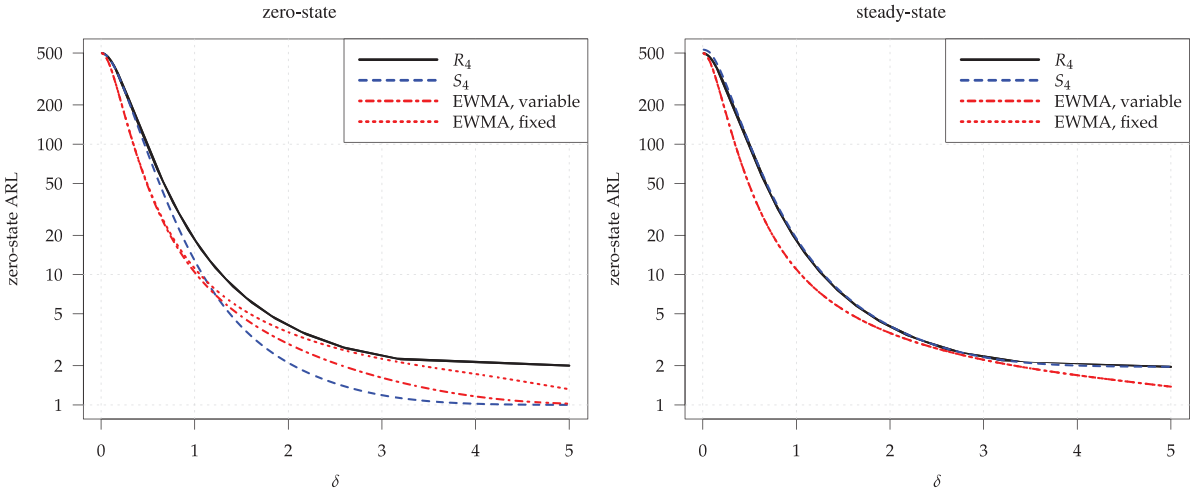

FIGURE 5 ARL envelopes (point-wise minimal, $ARL \to \min_{1 \le H \le 200}$) of R_4 and S_4 (also called AR and MSS); with in-control ARL 500; and the EWMA chart with $\lambda = 0.25$

configurations with $H \in \{2, 3\}$, low values for $E_1(L) = D_1, D_2$, and (only for S_4) D_3. But for every change after $\tau = 3$, the EWMA ($\lambda = 0.25$) chart beats all other optimized charts under study. Thus, synthetic-type charts could be recommended only for the special situation of early changes ($\tau \le 3$) with considerable magnitude ($\delta \ge 2$). Otherwise the classical EWMA chart with a mid-size $\lambda = 0.25$ is a better choice. Taking the ARL of the Shewhart chart into account, we conjecture that even a combination of synthetic-type charts and Shewhart charts, called "improved synthetic charts" in Rakitzis et al.,[7] will not be much better for changes $\delta < 2$. Before we provide our final judgment, however, some more comparisons (for a larger set of δ values) focusing on zero- and steady-state ARL will be considered. To make the presentation more concise, we focus on type #4 charts, that is, AR and MSS or R_4 and S_4, respectively. We include as well the no head-start version (AR) proposed by Antzoulakos and Rakitzis.[25]

To allow some overall judgment, we calculated ARL envelopes (Dragalin[39]) for R_4 and S_4. In detail, for each δ (on a rather fine grid), we pick H making the related out-of-control ARL minimal. The corresponding ARL values form the R_4 and S_4 envelope, respectively. In Table 3, we present some examples for these H values.

We obtained the results by searching over $H \in \{1, 2, \dots, 200\}$. Because for small and mid-size δ, the ARL minimum is achieved with quite large H while simultaneously the changes from $H = 5$ on are nearly negligible, we replace the "global" H by the smallest member of the above set, where the corresponding ARL is not larger by 0.1% than the overall minimum. We deployed the same approach for the values given in Figures 2–4 for S_4. It is not surprising that R_4 and S_4 have nearly the same optimal H values. Additionally, aiming at small zero- and steady-state ARLs results in similar H choices. In Appendix B, we provide in Figure B.1, two diagrams illustrating the dependence of the optimal H on δ in a more elaborate way. Here we want to emphasize that the actual choice of H is not important, as long as it is not too small. Thus, some choice such that $5 \le H \le 10$ does the job sufficiently well. For the envelope, however, we use the best choice over $H \in \{1, 2, \dots, 200\}$.

Turning now to Figure 5 presenting the envelopes, we want to note that besides the already utilized EWMA chart with alarm rule (2), we deploy as well an EWMA chart with constant limits, namely with alarm limit based on $\tilde{c}_E \sqrt{\lambda/(2-\lambda)}$ relying on the asymptotic standard deviation of the EWMA statistics. Thereby, the factor $\tilde{c}_E = 2.998$ is slightly smaller than

$c_E = 3.001$ in Equation (2) for the same in-control zero-state ARL ($A = 500$). The fixed limits EWMA as the competitor of R_4 is more popular in the SPM literature and related software packages, because obtaining the ARL is more feasible numerically. In Figure 5, we consider $0 < \delta \leq 5$.

From the envelope diagram for the zero-state ARL, we may conclude that synthetic-type charts, here S_4 in particular, perform well for change sizes $\delta > 1$. These statements, however, are only valid for the head-start versions S_i. From Figures 2–4, we know that this advantage vanishes as soon the change does not take place during the first few (less than 10) observations. That is, for most of the change point positions, the steady-state ARL is much more representative.

From the corresponding ARL envelope on the right-hand side of Figure 5, we conclude that the EWMA chart with $\lambda = 0.25$ uniformly dominates the **point-wise** best R_4 and S_4 configurations. Now the charts with head-start (S_4, EWMA with Equation (2) limits) and without head-start (R_4, EWMA with fixed limits) behave alike. Interestingly, the steady-state ARL values for $2 \leq \delta \leq 3$ do not differ considerably between EWMA and the #4 charts. But for smaller **and** larger values of δ, the EWMA chart performs much better than R_4/S_4. While there is some remedy for the large values of δ, nothing helps to improve the synthetic-type charts for changes smaller than $\delta \leq 2$. The dominating competitor is a standard EWMA chart with $\lambda = 0.25$, which could be further tuned to improve either the performance for smaller or larger δ. We note that changes of size $\delta \geq 3$ constitute the realm of Shewhart control charts. In summary, synthetic-type charts (here #4) feature good detection performance for mid-size changes, but are uniformly dominated by common EWMA control charts and partially overshadowed by Shewhart charts.

Next, we want to deal with the combination of synthetic-type charts and Shewhart charts, which was proposed in Rakitzis et al.,[7] and earlier in Wu et al.[38] and Shongwe and Graham.[19] As we will later see, this combination improves the out-of-control steady-state ARL results for $\delta > 3$, helping to close the gap between the right-hand portions of the curves in Figure 5. The adoption of the Markov chain models applied for all synthetic-type charts for incorporating the Shewhart limit is straightforward.[19,40] It is more difficult for Shewhart–EWMA (CSEWMA) charts, but the Markov chain approximation described in Lucas and Saccucci[8] works sufficiently well. We used the more accurate algorithm introduced by Capizzi and Masarotto.[9]

In order to illustrate the potential impact of adding the Shewhart rule, we consider for R_4 and S_4 the case $H = 6$, which is a reasonably general choice. Besides the above single EWMA charts with $\lambda = 0.25$ (exact and fixed limits), we consider a Shewhart–EWMA combination with $\lambda = 0.25$, Shewhart limit $k_2 = 3.25$, and EWMA threshold $\tilde{c}_E = 3.2097$ (in-control ARL 500), where the EWMA component features constant limits (otherwise ARL calculation becomes more complicated). For the two synthetic-type charts, we considered many combinations of (k_1, k_2), where k_1 replaces k in Equation (4) and k_2 is again the Shewhart limit (of course, $k_2 > k_1$). We started with $k_2 = 3.1$ (the limit for a standalone Shewhart chart with in-control ARL 500 is $k_2 = 3.09$) and increased it by 0.02 steps (up to 7). The k_1 of the inner synthetic rule was determined (for $H = 6$) to obtain the in-control zero-state ARL 500 for the combination. The resulting bundles of Shewhart-#4 charts provide the gray areas in Figure 6, where two members are highlighted.

The black solid line marks the original pure #4 chart, whereas the blue dashed lines represents an optimal member. Optimal means here that the measure $EQL = 1/\delta_{\max} \sum_i \delta_i^2 ARL_i$ is minimized (ARL_i is the out-of-control ARL for shift δ_i). The utility function EQL was used in Shongwe and Graham[19] in order to evaluate the detection performance over a range of shifts with a single number. We set $\delta_{\max} = 5$ and $\delta_i = 0.01i$. The impact of small shifts (our $\delta_1 = 0.01$ is small) to EQL is rather minuscule because of the weights δ_i^2. The resulting Shewhart limits k_2 are 4.78 for S_4 in case of the zero-state ARL, 3.46 in case of the steady-state ARL, and 3.48 for R_4 in both cases. Only the first value, $k_2 = 4.78$ sticks out, which is not surprising because the zero-state performance of the head-start scheme S_4 is already sound. The other values are quite similar. For R_4, it is not important what ARL measure is utilized. We recognize the improvement potential for shifts $\delta \geq 3$ (the Shewhart realm). The best Shewhart-#4 charts exhibit profiles that are slightly lifted for changes $\delta \leq 2$ and substantially lowered for $\delta \geq 3$. For the Shewhart-R_4 combination we observe quite similar patterns for the zero-state and the steady-state ARL. It is different for Shewhart-S_4, where many members of the aforementioned Shewhart-S_4 family yield small ARL values for $\delta > 1$.

We notice as well that the standalone EWMA chart with exact limits, see Equation (2), exhibits the best uniform performance among the EWMA charts. The other two involve constant limits, which results in higher zero-state ARL values by construction. However, the more interesting comparison is the one for the steady-state ARL. Here we conclude that all three EWMA designs behave better for changes $\delta < 2$, again. For changes $2 \leq \delta \leq 3$, all considered charts perform similarly.

We conclude for large changes, $\delta > 3$, that the combination schemes (Shewhart-#4 and Shewhart–EWMA) are the best ones and display roughly the same performance. Then the two standalone EWMA charts follow, as we observed already in Figure 5. The worst chart types are the standalone #4 charts (R_4/S_4). In summary, the merger of Shewhart

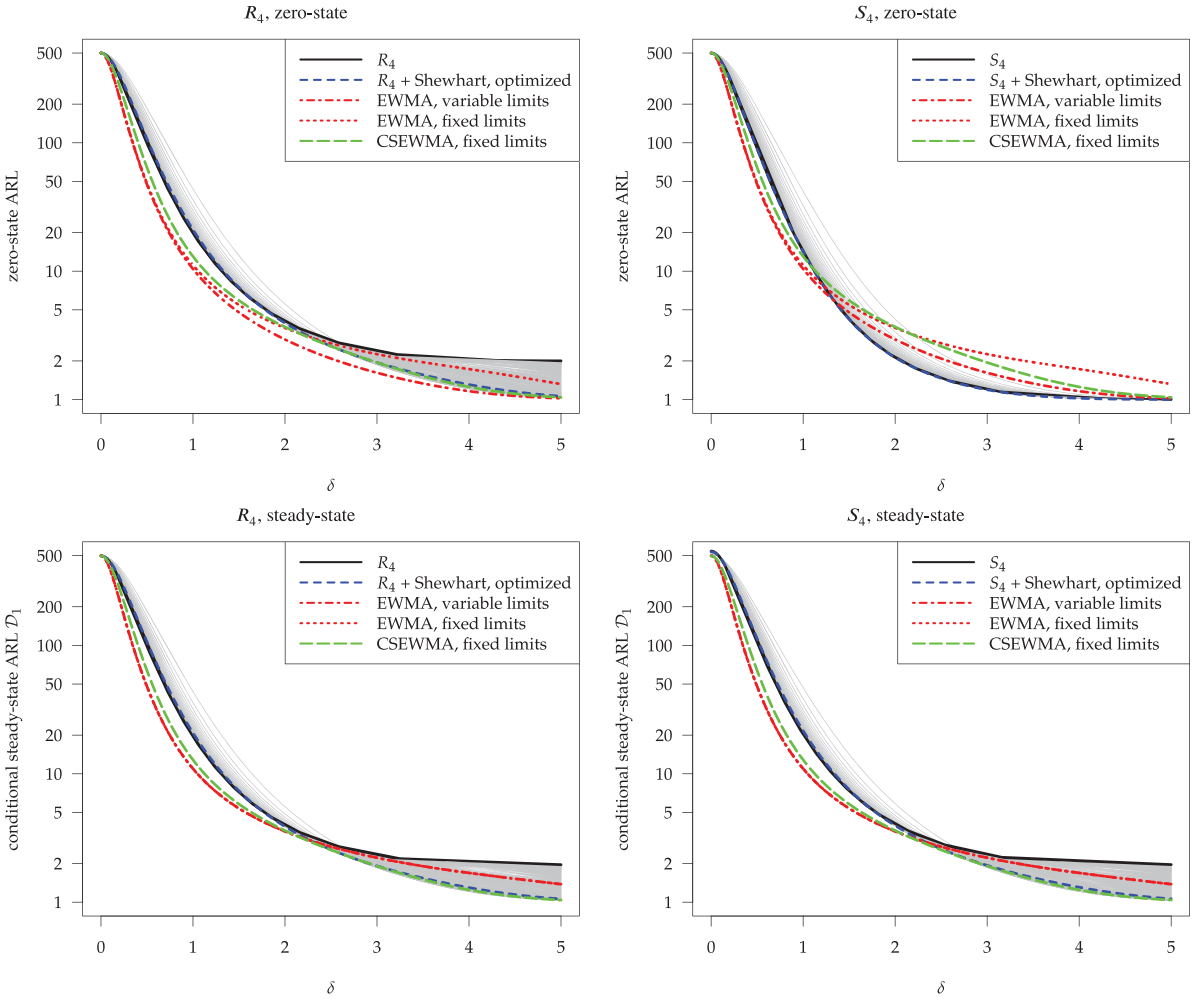

FIGURE 6 ARL performance of single charts and combinations; #4 charts with $H = 6$, EWMA chart(s) with $\lambda = 0.25$. In-control ARL 500

limits with synthetic-type charts helps to close the $\delta > 3$ ARL gap. However, the Shewhart–EWMA combination shows much better performance for changes $\delta \leq 2$, whereas for larger changes, it behaves like the optimal Shewhart-#4. Thus, a clear recommendation could be given: use either the single EWMA chart or the Shewhart–EWMA combination charts.

Finally, we want to stress the expedience of choosing the so-called wildcard head-start in contrast to the standard set up, which was chosen for the R_i charts, namely DR, KL, MC1, and AR by Derman and Ross,[22] Klein,[23] Machado and Costa,[24] and Antzoulakos and Rakitzis,[25] respectively. While the majority of the runs rules chart literature picked this initial state, which resembles the worst case (maximum out-of-control ARL), Wu and Spedding[1] started a movement to chose the best-case state. In Figure 7, we illustrate, how quickly these control charts "return" to the worst case after starting in the best-case.

For an in-control ARL of 500 ,we plot the probability that after i observations the synthetic chart arrives in the worst-case state. With $\mathfrak{S}_i$, we denote the state at observation i including $\mathfrak{S}_0$ as the initial state of the chart. From Table 2, we know the number of possible states (for the simple #1 chart, we observe 0 and H as best- and worst-case state following the notation in Equation (4), that is, picking the states from the set $\{0, 1, \ldots, H\}$). To improve presentation, we started plotting at this i, where the probability is greater than zero. Interestingly, for S_1, S_2, and S_3, we obtain $P(\mathfrak{S}_i = \text{worst-case} \mid L > i) = 0$ for $i < H$ and $P(\mathfrak{S}_H = \text{worst-case} \mid L > H) = 1$. If there is no (false) alarm during the first H observations, then we reach the worst-case state with probability 1 at the Hth observation. Thus, the behavior of the head-start ($\mathfrak{S}_0 = 0$ in case of S_1) and no-head-start design ($\mathfrak{S}_0 = H$ in case of R_1) differs substantially only during the first H observations. Then the head-start type chart arrives in the worst-case state with (conditional) probability one. The other chart started in the worst case (again $\mathfrak{S}_0 = H$ for R_1) with probability one, but returns to it at index H with a (conditional) probability, which is quite

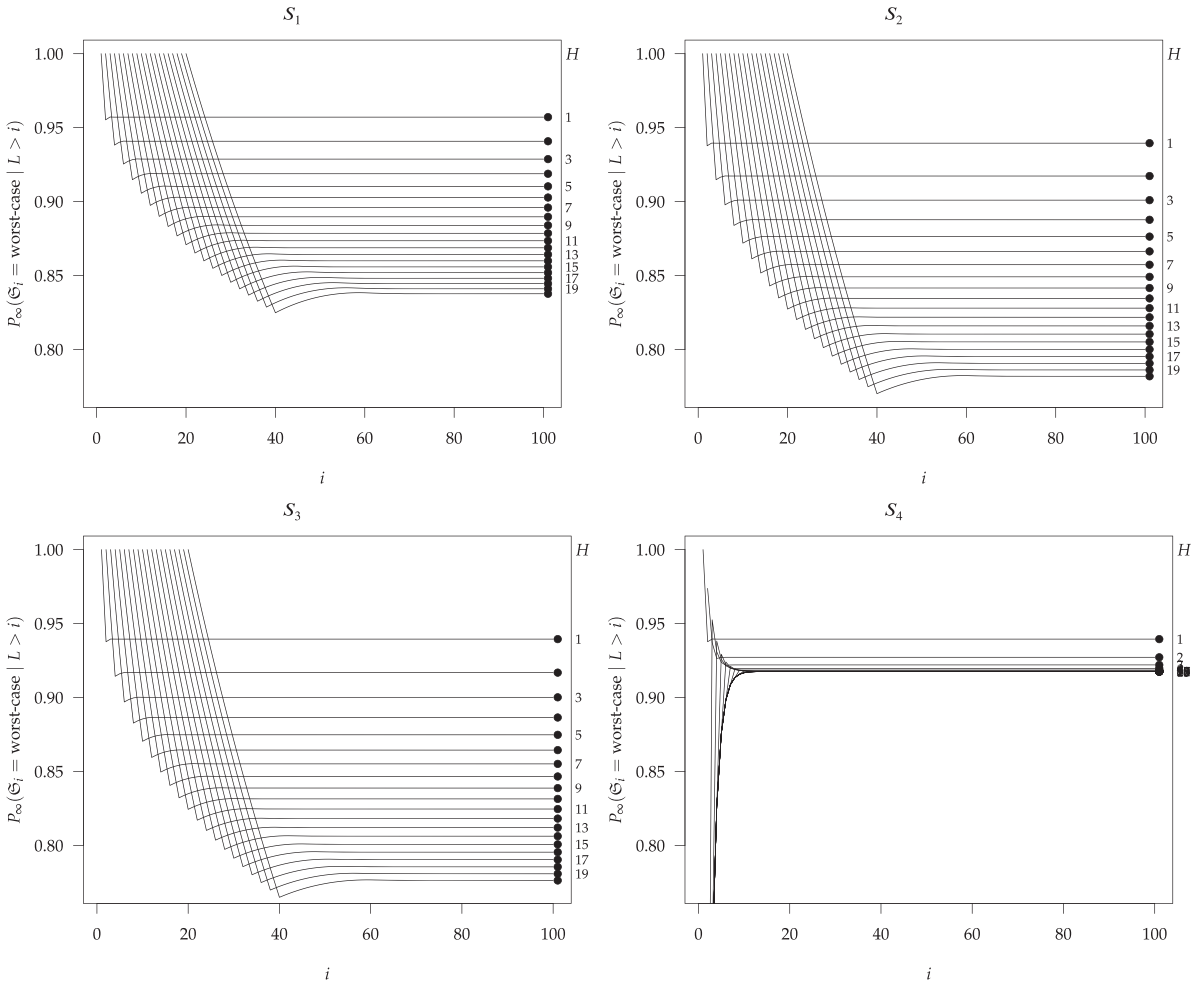

FIGURE 7 Conditional (in-control) probability of being in the worst-case state, $P_\infty(\mathfrak{S}_i = \text{worst-case} \mid L > i)$ (in case of S_1 just $\mathfrak{S}_i = H$) with zero portions skipped, $i = 1, 2, \ldots, 100$; in-control ARL 500, $H = 1, 2, \ldots, 20$

large, but smaller than one. The bullets at the end of all profiles in Figure 7 mark the conditional steady-state probability of the worst case. For all four chart types and all considered $H = 1, 2, \ldots, 20$ the convergence to the latter values is quick.

The S_4 chart differs slightly from the other ones. First, only for $H = 1$, we observe $P(\mathfrak{S}_H = \text{worst-case} \mid L > H) = 1$. For larger H, we neither get long series of zero probabilities (from $i = 2$ on the probability is positive) nor the probability one at $i = H$. But more importantly, the dominating probability value is about 92%. Thus the best design among all considered synthetic-type charts with head-start, namely S_4, exhibits two features: (i) it reveals excellent zero-state ARL results, cf. to Figure 5. (ii) These low values are highly untypical facets of S_4, because it operates with a probability of more than 90% in worst-case mode. Thus, a thorough and legitimate judgment of the S_4 chart would rely on the ARL values we know for the no head-start version, that is, for R_4. Another way of avoiding misjudgment is, of course, considering the steady-state ARL. Finally we should mention that a similar statement could be given for S_1, S_2, and S_3, because the probability of being in the worst case (for $i \geq H$) is not much smaller, it is for all considered configurations larger than 75%.

5 | CONCLUSIONS

Of course, simple runs-rule-based synthetic-type charts ($R_1, S_1, \ldots, R_4, S_4$) are easy to build and to analyze. In particular, for the run-length analysis, one can easily apply exact Markov chain models. For the simplest ones, R_1 and S_1, there are even explicit solutions for all considered measures. Recall that the zero-state ARL results for R_1 have been known since Page.[16] EWMA control charts, however, are similarly easy to use. Their ARL analysis needs more computational power, which is not a problem nowadays. Given the results in Section 4, we can extend the criticism from Knoth[6] to the new

synthetic-type schemes advocated in Rakitzis et al.[7] Detection performance-wise, a clear recommendation can be given competing with all eight synthetic-type charts: apply the EWMA chart, because it exhibits the best detection performance for small changes $\delta \leq 1.5$ (in terms of standard deviation) in our study, whereas for larger changes, all the considered schemes behave similarly. See Woodall and Faltin[41] for some discussion of choosing appropriate shift ranges while setting up a control chart.

Without an added Shewhart rule, synthetic-type charts perform worse than the EWMA chart even for large changes ($\delta > 3$). Adding this Shewhart rule improves the large change detection behavior considerably, for both synthetic-type (here we focus to R_4 and S_4, the most recent phenotypes) and EWMA control charts. It turned out that these "improved synthetic charts" are not completely new, because already Page[16] investigated R_1 providing explicit ARL results. We demonstrated, however, that Shewhart–EWMA chart combinations provide uniformly better (detecting changes more quickly) steady-state ARL performance (for $\delta < 2$ considerably better and for $\delta \geq 2$ slightly better) than all investigated "improved" R_4 and S_4 charts, which are the best synthetic-type charts.

The R_i charts can be designed through the lens of their worst-case ARL. In Appendix C, a rough comparison between R_4 and cumulative sum charts (CUSUM) introduced in Page[33] is provided. Again, the older charts (CUSUM) yield better ARL results. In summary, simple runs-rule-based synthetic-type charts are somewhat easier to set up than the classical charts such as EWMA and CUSUM, but the older ones exhibit the better detection performance.

Finally, we want to emphasize that for a sound analysis of control chart performance, one must consider the steady-state ARL. Naturally, a worst-case ARL analysis would be appropriate too.

DATA AVAILABILITY STATEMENT

Data sharing not applicable to this article as no datasets were generated or analyzed during the current study.

ORCID

Sven Knoth https://orcid.org/0000-0002-9666-5554

References

1. Wu Z, Spedding TA. A synthetic control chart for detecting small shifts in the process mean. *J Qual Technol*. 2000;32(1):32-38. https://doi.org/10.1080/00224065.2000.11979969
2. Wu Z, Spedding TA. Implementing synthetic control charts. *J Qual Technol*. 2000;32(1):74-78. https://doi.org/10.1080/00224065.2000.11979973
3. Shewhart WA. The application of statistics as an aid in maintaining quality of a manufactured product. *J Am Statist Assoc*. 1925;20(152):546-548. https://doi.org/10.1080/01621459.1925.10502930
4. Crosier RB. A new two-sided cumulative quality control scheme. *Technometrics*. 1986;28(3):187-194. https://doi.org/10.2307/1269074
5. Davis RB, Woodall WH. Evaluating and improving the synthetic control chart. *J Qual Technol*. 2002;34(2):200-208. https://doi.org/10.1080/00224065.2002.11980146
6. Knoth S. The case against the use of synthetic control charts. *J Qual Technol*. 2016;48(2):178-195. https://doi.org/10.1080/00224065.2016.11918158
7. Rakitzis AC, Chakraborti S, Shongwe SC, Graham MA, Khoo MBC. An overview of synthetic-type control charts: techniques and methodology. *Qual Reliab Eng Int*. 2019;35(7):2081-2096. https://doi.org/10.1002/qre.2491
8. Lucas JM, Saccucci MS. Exponentially weighted moving average control schemes: properties and enhancements. *Technometrics*. 1990;32(1):1-12. https://doi.org/10.1080/00401706.1990.10484583
9. Capizzi G, Masarotto G. Evaluation of the run-length distribution for a combined Shewhart–EWMA control chart. *Stat Comput*. 2010;20(1):23-33. https://doi.org/10.1007/s11222-008-9113-8
10. Shongwe SC, Graham MA. A modified side-sensitive synthetic chart to monitor the process mean. *Qual Technol Quant Manag*. 2018;15(3):328-353. https://doi.org/10.1080/16843703.2016.1208939
11. Shewhart WA. *Contributions of Statistics to the Science of Engineering*. University of Pennsylvania Press; 1941:97-124.
12. Dudding BP, Jennett WJ. *Quality Control Charts*. British Standards Institution; 1942.
13. Wolfowitz J. On the theory of runs with some applications to quality control. *Annals of Mathematical Statistics*. 1943;14:280-288. https://doi.org/10.1214/aoms/1177731421
14. Weiler H. The use of runs to control the mean in quality control. *J Am Statist Assoc*. 1953;48(264):816-825. https://doi.org/10.1080/01621459.1953.10501203
15. Weiler H. A new type of control chart limits for means, ranges, and sequential runs. *J Am Statist Assoc*. 1954;49(266):298-314. https://doi.org/10.1080/01621459.1954.10483506
16. Page ES. Control charts with warning lines. *Biometrika*. 1955;42(1-2):243-257. https://doi.org/10.1093/biomet/42.1-2.243
17. WECO. *Statistical Quality Control Handbook*. Western Electrical Company (WECO); 1956.
18. Moore PG. Some properties of runs in quality control procedures. *Biometrika*. 1958;45(1/2):89-95.

19. Shongwe SC, Graham MA. On the performance of Shewhart-type synthetic and runs-rules charts combined with an $\bar{X}$ chart. *Qual Reliab Eng Int*. 2016;32(4):1357-1379. https://doi.org/10.1002/qre.1836
20. Bersimis S, Koutras MV, Rakitzis AC. Run and scan rules in statistical process monitoring. In: Glaz J, Koutras MV, eds. *Handbook of Scan Statistics*. Springer; 2020:1-32.
21. Shongwe SC, Graham MA. Some theoretical comments regarding the run-length properties of the synthetic and runs-rules $\bar{X}$ monitoring schemes – part 2: steady-state. *Qual Technol Quant Manag*. 2019;16(2):190-199. https://doi.org/10.1080/16843703.2017.1389142
22. Derman C, Ross SM. *Statistical Aspects of Quality Control*. Academic Press; 1997.
23. Klein M. Two alternatives to the Shewhart $\bar{X}$ control chart. *J Qual Technol*. 2000;32(4):427-431. https://doi.org/10.1080/00224065.2000.11980028
24. Machado MAG, Costa AFB. Some comments regarding the synthetic $\bar{X}$ Chart. *Commun Stat Theory Methods*. 2014;43(14):2897-2906. https://doi.org/10.1080/03610926.2012.683128
25. Antzoulakos DL, Rakitzis AC. The modified *r* out of *m* control chart. *Commun Stat Simul Comput*. 2008;37(2):396-408. https://doi.org/10.1080/03610910701501906
26. Chakraborti S, Rakitzis AC. Wiley StatsRef: statistics reference online. Control charts, synthetic. 2021:1-18. https://doi.org/10.1002/9781118445112.stat08340
27. Roberts SW. Control chart tests based on geometric moving averages. *Technometrics*. 1959;1(3):239-250. https://doi.org/10.1080/00401706.1959.10489860
28. Montgomery DC. *Introduction to Statistical Quality Control*. Wiley; 2019.
29. Crowder SV. A simple method for studying run-length distributions of exponentially weighted moving average charts. *Technometrics*. 1987;29(4):401-407. https://doi.org/10.1080/00401706.1987.10488267
30. Knoth S. EWMA schemes with non-homogeneous transition kernels. *Seq Anal*. 2003;22(3):241-255. https://doi.org/10.1081/SQA-120025169
31. Knoth S. Fast initial response features for EWMA control charts. *Stat Papers*. 2005;46(1):47-64. https://doi.org/10.1007/BF02762034
32. Knoth S. *spc: Statistical Process Control - Collection of Some Useful Functions*. R Foundation for Statistical Computing; 2021. R package version 0.6.5.
33. Page ES. Continuous inspection schemes. *Biometrika*. 1954;41(1-2):100-115. https://doi.org/10.1093/biomet/41.1-2.100
34. Taylor HM. The economic design of cumulative sum control charts. *Technometrics*. 1968;10(3):479-488. https://doi.org/10.1080/00401706.1968.10490595
35. Knoth S. Steady-state average run length(s) – methodology, formulas and numerics. *Seq Anal*. 2021;40(3):405-426. https://doi.org/10.1080/07474946.2021.1940501
36. Brook D, Evans DA. An approach to the probability distribution of CUSUM run length. *Biometrika*. 1972;59(3):539-549. https://doi.org/10.2307/2334805
37. Darroch JN, Seneta E. On quasi-stationary distributions in absorbing discrete-time finite markov chains. *J Appl Probab*. 1965;2(1):88-100. https://doi.org/10.2307/3211876
38. Wu Z, Ou Y, Castagliola P, Khoo MB. A combined synthetic $\bar{X}$ chart for monitoring the process mean. *Int J Prod Res*. 2010;48(24):7423-7436. https://doi.org/10.1080/00207540903496681
39. Dragalin V. Optimal CUSUM envelope for monitoring the mean of normal distribution. *Econ Qual Control*. 1994;9(4):185-202.
40. Shongwe SC, Graham MA. Synthetic and runs-rules charts combined with an $\bar{X}$ chart: theoretical discussion. *Qual Reliab Eng Int*. 2017;33(1):7-35. https://doi.org/10.1002/qre.1987
41. Woodall WH, Faltin FW. Rethinking control chart design and evaluation. *Qual Eng*. 2019;31(4):596-605. https://doi.org/10.1080/08982112.2019.1582779
42. Knoth S. New results for two-sided CUSUM-Shewhart control charts. In: Sven K, Wolfgang S, eds. *Frontiers in Statistical Quality Control 12*. Springer International Publishing; 2018:45-63.

AUTHOR BIOGRAPHY

Sven Knoth is a Professor of Statistics in the Department of Mathematics and Statistics within the School of Economic and Social Sciences at the Helmut Schmidt University, Hamburg, Germany. Prior to that, he worked as a Senior SPC Engineer at Advanced Mask Technology Center (AMTC) Dresden, Germany, from 2004 to 2009. He is an Associate Editor of Computational Statistics.

How to cite this article: Knoth S. An expanded case against synthetic-type control charts. *Qual Reliab Eng Int*. 2022;38:3197–3215. https://doi.org/10.1002/qre.3128

APPENDIX A: EXPLICIT FORMULA FOR STEADY-STATE ARL FOR S_1 (R_1) AND ITS LIMIT FOR $\delta \to 0$

Because in Shongwe and Graham,[19] the steady-state ARL was deployed to determine the control chart limit k, we consider the simplest case, namely S_1 (and implicitly R_1) more thoroughly, augmenting the results in Shongwe and Graham.[21,40] We consider all ψ_i, $i = 1, 2, 3, 4$ (see Section 3). The shift δ is added as a subscript; for example $\boldsymbol{\psi}_{1;0}$ denotes the in-control case $\delta = 0$.

Conditional steady-state ARL, cf. to Knoth[6]

$$\mathscr{D}_1 = \boldsymbol{\psi}'_{1;0}\,\boldsymbol{\ell}_\delta = \left(\frac{\varrho_0}{p_0} + \frac{1-\left(\frac{q_0}{\varrho_0}\right)^H}{1-\frac{q_0}{\varrho_0}}\right)\frac{s_0}{p_\delta} + \left(\frac{\varrho_0}{p_0} + q_\delta^H\frac{1-\left(\frac{q_0}{q_\delta\varrho_0}\right)^H}{1-\frac{q_0}{q_\delta\varrho_0}}\right)\frac{s_0}{r_\delta} \quad \xrightarrow{\delta\to 0} \quad \frac{1}{1-\varrho_0}.$$

Cyclical steady-state ARL, restart at state 0, cf. to Wu et al.[38,6]

$$\mathscr{D}_2 = \boldsymbol{\psi}'_{2;0}\,\boldsymbol{\ell}_\delta = \frac{1+q_0p_\delta\frac{q_0^H-q_\delta^H}{q_0-q_\delta}}{r_\delta} \quad \xrightarrow{\delta\to 0} \quad \frac{1+Hp_0q_0^H}{r_0} = \frac{1}{r_0} + H\frac{q_0^H}{1-q_0^H}.$$

Cyclical steady-state ARL, restart at state H, cf. to Shongwe and Graham[21]

$$\mathscr{D}_3 = \boldsymbol{\psi}'_{3;0}\,\boldsymbol{\ell}_\delta = \frac{1-q_\delta^H}{r_\delta} + \frac{1+p_0q_\delta\frac{q_0^H-q_\delta^H}{q_0-q_\delta}}{r_\delta\left(2-q_0^H\right)} \quad \xrightarrow{\delta\to 0} \quad \frac{1-q_0^H}{r_0} + \frac{1+Hp_0q_0^H}{r_0\left(2-q_0^H\right)}.$$

Wrong conditional steady-state ARL, cf. to Shongwe and Graham[40,21]:

$$\mathscr{D}_4 = \boldsymbol{\psi}'_{4;0}\,\boldsymbol{\ell}_\delta = \frac{1-q_\delta^H}{r_\delta} + \frac{1+p_0q_\delta\frac{1-q_\delta^H}{1-q_\delta}}{r_\delta(1+Hp_0)} \quad \xrightarrow{\delta\to 0} \quad \frac{1-q_0^H}{r_0} + \frac{1+q_0\left(1-q_0^H\right)}{r_0(1+Hp_0)}.$$

Next we apply the above formulas for a S_1 chart with $H = 3$ and $k = 2.2238$ (in-control ARL 500). Besides the four different steady-state ARL results, we show as well the zero-state ARL of an R_1 (the true synthetic chart without head-start) in the following Table A.1.

The four $\mathscr{D}_i$ values are nearly the same. Thus, using one of the correct or even the wrong ($\mathscr{D}_4$) formulas makes little difference. Interestingly, the zero-state ARL ℓ_{R_1} chart is close to these values as well. Thus, for charts without a head-start, it is sufficient to consider the zero-state ARL (the mentioned behavior carries over to the out-of-control case).

To judge this behavior for the out-of-control case, we plotted some $\mathscr{D}_i$ profiles in Figure A.1. Not surprisingly, all these profiles coincide. From these values, we conclude that the incorrect steady-state vector approach in Shongwe and Graham[21,40] works well.

We mention that calibrating (setting k for synthetic-type charts) control charts to achieve a certain in-control steady-state ARL, as it was done in Shongwe and Graham,[19] refers to starting the chart from its steady-state distribution. This is certainly not a common approach in SPM practice.

TABLE A.1 In-control ARL for S_1 and R_1, zero-state ℓ and steady-state $\mathscr{D}$, $H = 3$, $k = 2.2238$

ℓ_{S_1}	ℓ_{R_1}	$\mathscr{D}_1$	$\mathscr{D}_2$	$\mathscr{D}_3$	$\mathscr{D}_4$
500	538.224	536.378	536.242	536.383	536.354

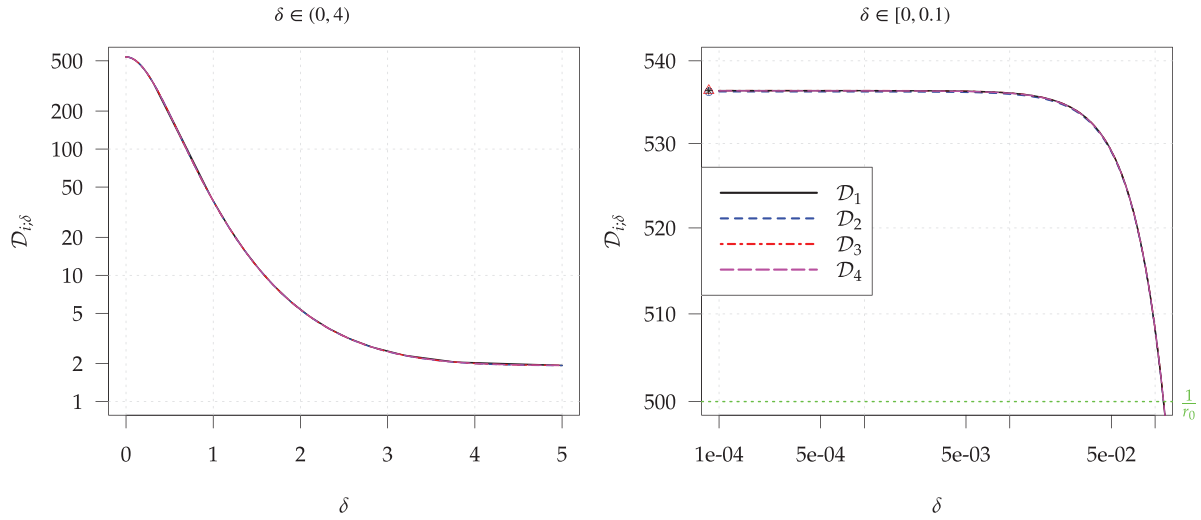

FIGURE A.1 Various types of steady-state ARL, $\mathcal{D}_i$, for a typical range of changes (0,5) and for $\delta \to 0$, true synthetic chart with head-start (S_1) with $H = 3$ and $k = 2.2238$ (in-control ARL 500)

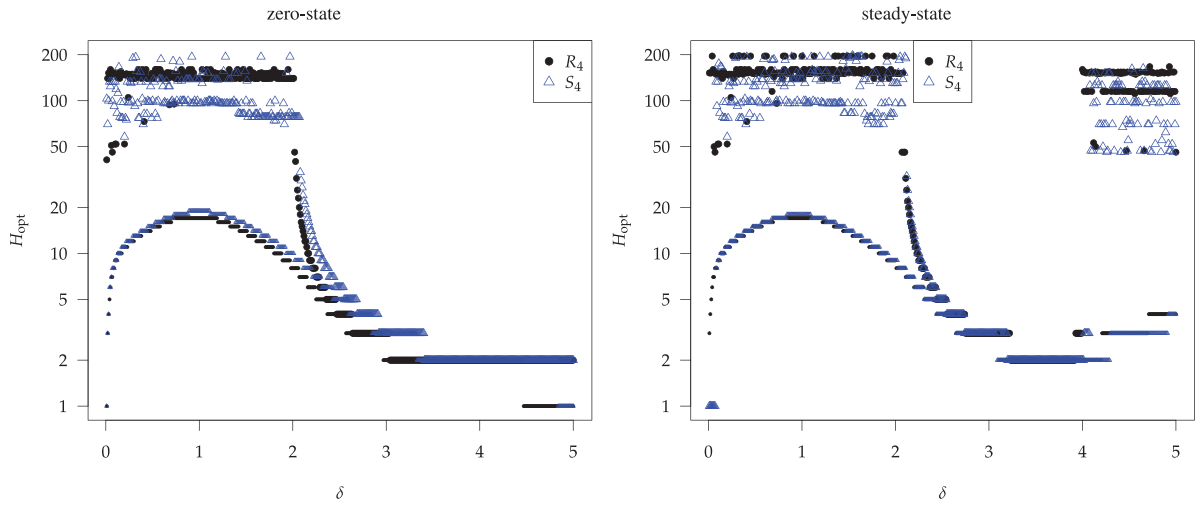

FIGURE B.1 Optimal H values

APPENDIX B: MINIMIZING OUT-OF-CONTROL ARL BY TUNING *H*

In addition to the values given in Table 3 (Section 4), we show here the complete output of our optimization procedure. For both #4 charts (R_4 and S_4) we tried $H \in \{1, 2, \ldots, 200\}$ and picked the H value that either minimizes the zero- or the steady-state ARL. In addition, we searched for small H values that yield ARL values not larger by 0.1% than the overall minimum. These H values are plotted in Figure B.1. The in-control ARL is set to 500. We observe quite similar patterns for both ARl metrics. The most pronounced difference can be seen for $\delta > 4$. Fortunately, tuning synthetic-type charts to detect such large changes is quite uncommon.

APPENDIX C: WORST-CASE ARL COMPETITION

Here, we compare the zero-state ARL of R_4 ($H = 8$—optimal for $\delta = 2$) and of two-sided CUSUM control charts. For the latter, we choose $k = 1$ (k denotes here the reference value of a CUSUM control chart) to achieve good performance for mid-size changes ($\delta = 2$ and its neighborhood).

We add as well a combination of R_4 and a Shewhart limit ($k_2 = 3.25$) to deal with the weak performance of R_4 for large shifts. The $k = 1$ CUSUM chart ($h = 2.665$) is uniformly better than R_4. Compared to R_4, the Shewhart-R_4 combination exhibits better detection performance for $\delta \geq 3$. Finally, the Shewhart-CUSUM combination ($k = 1$, $k_2 = 3.25$ and $h = 2.947$) shows lower out-of-control ARL results for $\delta < 3$ and more or less the same values for $\delta \geq 3$ as the

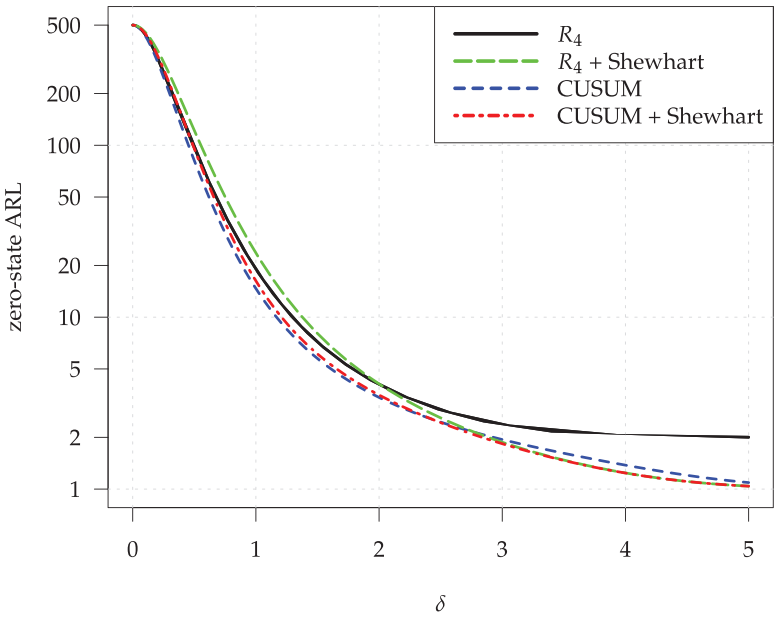

FIGURE C.1 Zero-state ARL comparison between R_4 ($H = 8$) and CUSUM control charts ($k = 1$). In-control ARL 500. For both a combination with a Shewhart chart (alarm threshold $k_2 = 3.25$) is included

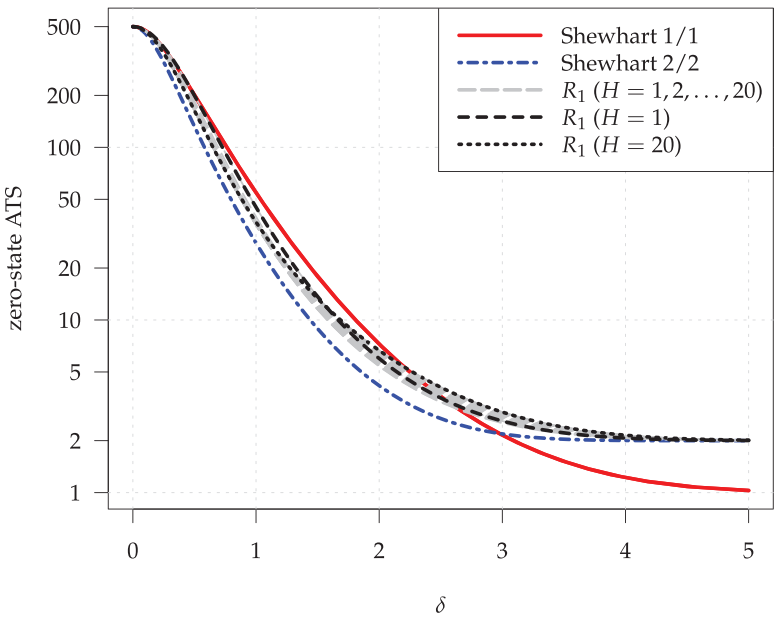

FIGURE C.2 Zero-state ATS comparison between R_1 ($H = 1, 2, \ldots, 20$) and two Shewhart control charts. In-control ARL 500

Shewhart-R_4 combination. Thus, the CUSUM schemes win both worst-case ARL competitions. The ARL values of the Shewhart-CUSUM combination were determined with the algorithms given in Knoth.[42] For the standard CUSUM, the function `xcusum.arl()` from the R package `spc` was used (Figure C.1).

Comparing the much simpler R_1 chart (primary synthetic chart, but without head-start) with the Shewhart chart in two sampling modes (every sampling point one observation, every other point two observations) yields some surprising insights. In order to deal with the two sampling patterns, we apply the (zero-state) average time to signal (ATS = ARL $\times$ sampling points between two succeeding observations). In Figure C.2, we present ATS profiles for $0 \leq \delta \leq 5$. To illustrate potential strengths and deficiencies of R_1, we consider $H = 1, 2, \ldots, 20$, whereas the two extremes are highlighted. Interestingly, the Shewhart chart (2/2 in Figure C.2) that collects every other sampling point two observations (or just calculates every other point the average of the last two observations) shows uniformly smaller ATS values than all examined R_1 chart designs. Thus, the primary synthetic chart is dominated by a Shewhart chart, which aggregates two succeeding observations, if we consider the worst-case ATS (equal to the zero-state ATS of R_1).

APPENDIX D: FURTHER CED PROFILES

In addition to the cases $\delta \in \{1, 2, 3\}$, we show here some CED profiles for $\delta \in \{0.5, 1.5\}$. In both cases, the EWMA chart performance is the best (Figure D.2).

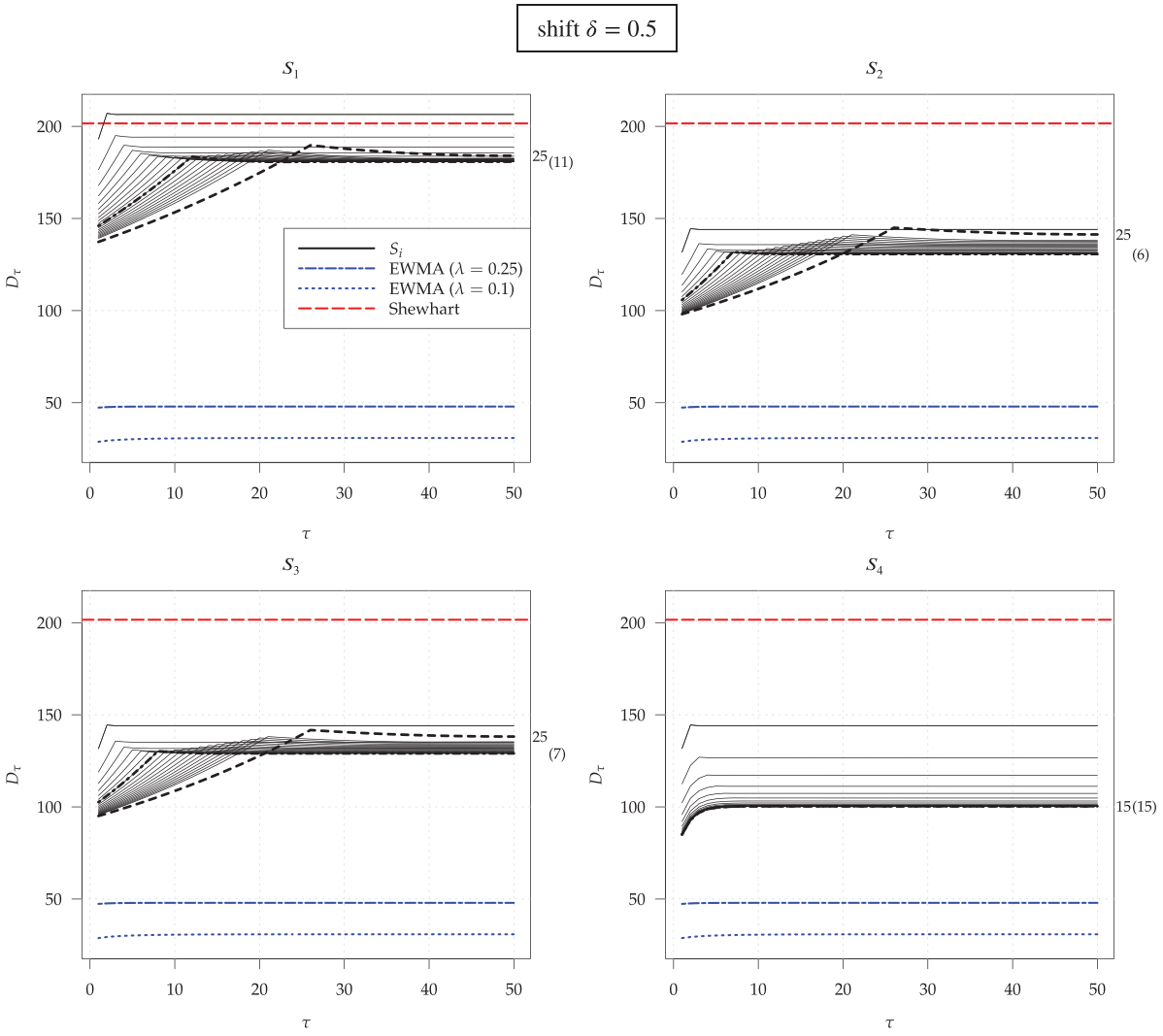

FIGURE D.1 CED profiles D_τ for four synthetic-type charts with head-start, with $H = 1, 2, \ldots, 20$. The best scheme (zero-state and steady-state) is bolded (dashed and dash-dotted) lines. Two EWMA charts are included. All with in-control ARL 500

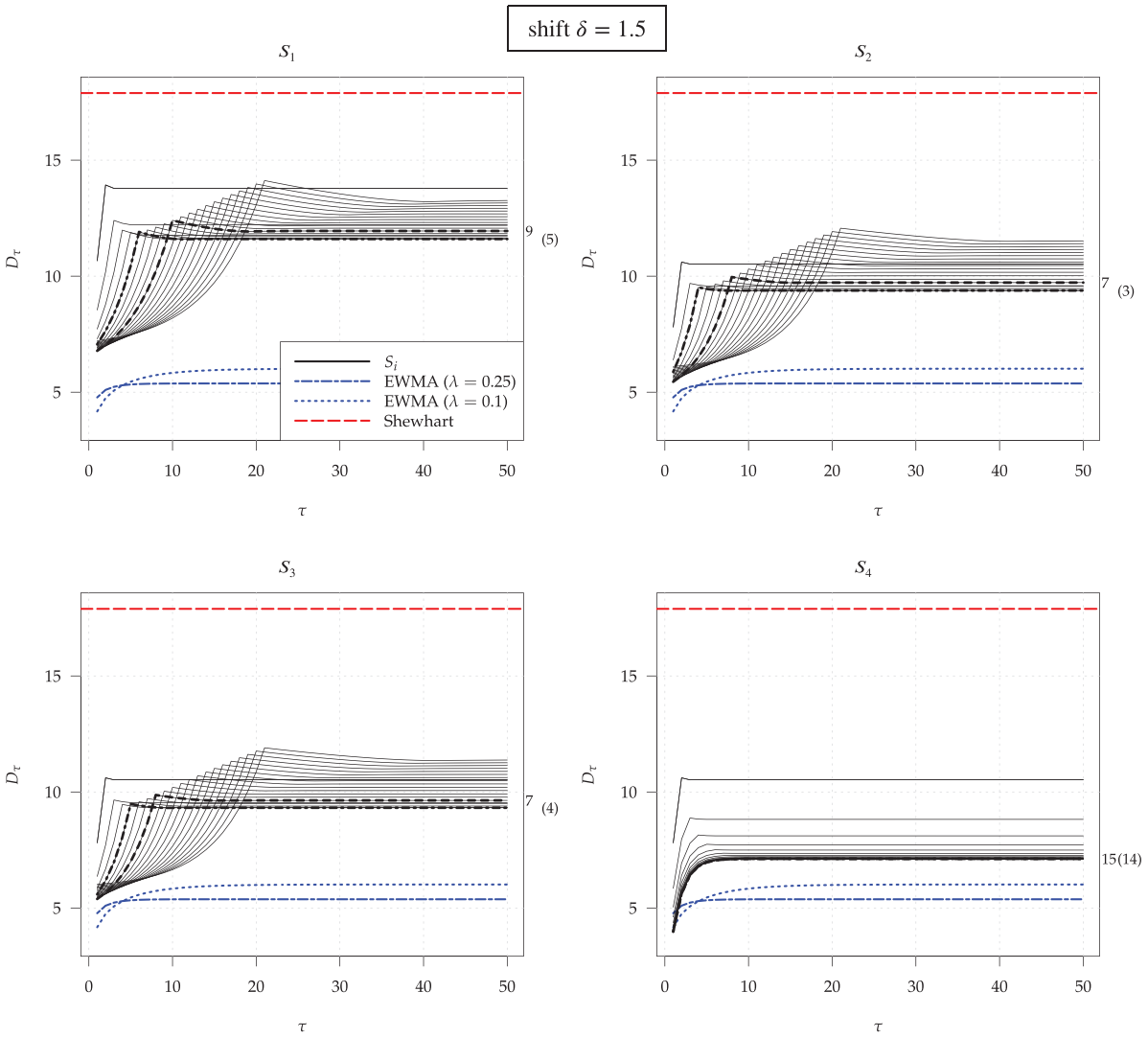

FIGURE D.2 CED profiles D_τ for four synthetic-type charts with head-start, with $H = 1, 2, \ldots, 20$. The best scheme (zero-state and steady-state) is bolded (dashed and dash-dotted) lines. Two EWMA charts are included. All with in-control ARL 500